Tracing hydrologic flow paths in a small forested watershed using variations in $^{87}Sr/^{86}Sr$, [Ca]/[Sr], [Ba]/[Sr] and $\delta^{18}O$

James F. Hogan[1] and Joel D. Blum[2]

Department of Earth Sciences, Dartmouth College, Hanover, New Hampshire, USA

Received 19 November 2002; accepted 22 July 2003; published 15 October 2003.

[1] Natural variations in $^{87}Sr/^{86}Sr$, [Ca]/[Sr], [Ba]/[Sr], and $\delta^{18}O$ were used to investigate changing hydrologic flow paths during storm events in an 11.8 ha first-order watershed of the Hubbard Brook Experimental Forest. Throughfall, soil water, and stream water were sampled during several storm events and a single snowmelt event. Throughfall had $^{87}Sr/^{86}Sr$, [Ca]/[Sr], and $\delta^{18}O$ values that were distinct from other water types. Soil water was highly variable in composition but could be separated into three distinct elevation zones in the watershed with $^{87}Sr/^{86}Sr$ and [Ba]/[Sr] both increasing with elevation in the watershed. Changes in $^{87}Sr/^{86}Sr$, [Ba]/[Sr], and $\delta^{18}O$ of stream water during storm events yielded complementary information about watershed hydrologic flow paths. Traditional hydrograph separation using $\delta^{18}O$ values indicated that new water was only a small component of storm flow (9–18%), whereas $^{87}Sr/^{86}Sr$ and [Ba]/[Sr] ratios indicated that shallow subsurface flow (soil water) contributed significantly to storm flow in amounts up to 40%, depending on soil moisture conditions. *INDEX TERMS:* 1860 Hydrology: Runoff and streamflow; 1040 Geochemistry: Isotopic composition/chemistry; 1045 Geochemistry: Low-temperature geochemistry; *KEYWORDS:* strontium isotopes, watershed hydrology, oxygen isotopes, runoff generation

Citation: Hogan, J. F., and J. D. Blum, Tracing hydrologic flow paths in a small forested watershed using variations in $^{87}Sr/^{86}Sr$, [Ca]/[Sr], [Ba]/[Sr] and $\delta^{18}O$, *Water Resour. Res.*, *39*(10), 1282, doi:10.1029/2002WR001856, 2003.

1. Introduction

[2] The pathways and transit times for the transport of precipitation to the stream channel are of fundamental importance in watershed hydrology. Oxygen and hydrogen isotopes are among the most widely applied tracers used to investigate these processes [*Kendall et al.*, 1995]. Most applications utilize variations in the isotopic composition of precipitation to calculate the relative contributions of precipitation (new water) and pre-event water (old water) to storm hydrographs [*Genereux and Hooper*, 1998]. A limitation with O and H isotopes is the lack of information about the path that water takes to reach the stream channel. For example, O isotopes generally cannot distinguish between pre-event groundwater and pre-event soil water, or between channel interception of throughfall and overland flow. Thus O and H isotopes separate time source components of streamflow, but often do not separate geographic source components [*Genereux and Hemond*, 1990; *Genereux and Hooper*, 1998]. Many studies, based on changes in stream solute chemistry in addition to O and H isotopes, have indicated that at least three flow paths (or end-member waters) contribute to storm flow [e.g., *Miller and Drever*, 1977; *Dewalle and Sharpe*, 1988; *Hooper et al.*, 1990; *Ogunkoya and Jenkins*, 1993; *Rice and Hornberger*, 1998].

[3] There are four main flow paths by which water can reach a stream channel: (1) overland flow, (2) shallow subsurface flow, (3) deeper subsurface flow under saturated conditions (hereafter referred to as groundwater flow), and (4) saturation overland flow, which includes both direct precipitation onto saturated areas (notably the stream channel) and return flow. Overland flow typically occurs only in arid or disturbed environments. In densely vegetated humid watersheds, most storm flow is generated by a combination of shallow subsurface flow and saturation overland flow [*Dunne*, 1978, 1982; *Hornberger et al.*, 1998]. These flow paths represent end-members based on mechanism, but in reality there is a full spectrum of flow path lengths and times [*Kirchner et al.*, 2000] as well as spatial and temporal changes in the areas and mechanisms that generate storm flow, known as the variable source area concept [*Hewlett and Hibbert*, 1967; *Dunne and Black*, 1970; *Dunne*, 1978, 1982]. Because of the complexity of these processes there is still considerable debate as to the mechanisms of storm flow generation in different hydrologic environments. In addition, understanding the exact nature of hydrologic flow paths is important for developing more realistic models of catchment hydrology, especially those for watershed acidification and biogeochemical cycling. For these reasons there is a need to develop additional tracers that are sensitive to these hydrologic flow paths. Natural variation in the isotopic and trace element ratios of solutes provides a potential means of tracing water flow paths within a watershed. If different flow paths (or water from different portions of the watershed) have distinct isotopic or solute ratios, then changes in flow path will be reflected by changes in the composition of the stream water. By combining solute ratios and solute isotopes with O or H isotopes, in a "multitracer approach," there is the

[1]Now at Department of Hydrology and Water Resources, University of Arizona, Tucson, Arizona, USA.

[2]Now at Department of Geological Sciences, University of Michigan, Ann Arbor, Michigan, USA.

0043-1397/03/2002WR001856

potential to enhance the understanding of watershed hydrology [*Kendall et al.*, 1995; *Bullen and Kendall*, 1998].

[4] One potentially useful solute isotope system is strontium. Because Sr isotopes are not fractionated significantly in nature (and if fractionation does occur it is corrected during data analysis) the $^{87}Sr/^{86}Sr$ ratio of dissolved Sr records only the $^{87}Sr/^{86}Sr$ ratio of the solute source(s). Natural variation in the $^{87}Sr/^{86}Sr$ ratio of rocks and soils results from the fact that ^{86}Sr is nonradiogenic whereas ^{87}Sr is produced by the decay of ^{87}Rb (half-life = 4.8×10^{10} yrs). The $^{87}Sr/^{86}Sr$ ratio of natural waters is mainly a reflection of Sr released through chemical weathering. Other processes, most notably atmospheric deposition [*Bullen and Kendall*, 1998], can also influence the Sr isotopic composition of water [*Miller et al.*, 1993; *Bailey et al.*, 1996].

[5] A limited number of studies have examined strontium isotope variability in small watersheds. In a series of nested catchments at the Sleepers River Research Watershed (Vermont), the $^{87}Sr/^{86}Sr$ ratio of stream water was found to systematically change with increasing basin size due to an increasing proportion of deep flow. Within each basin there was little variation in the $^{87}Sr/^{86}Sr$ ratio associated with changes in discharge, but subtle seasonal variations were observed [*Bullen and Kendall*, 1998]. At the Hauver Branch and Hunting Creek catchments (Maryland), variation in the $^{87}Sr/^{86}Sr$ ratio of stream water was positively correlated with changes in $\delta^{13}C$ values (DIC) during storm events and appears to record changing contributions of shallow groundwater and soil water from the unsaturated zone [*Bullen and Kendall*, 1998]. At Rowantree Burn in southern Scotland, analysis of two storm events showed no systematic variation in the $^{87}Sr/^{86}Sr$ ratio of stream water with changing discharge, even though the Sr concentration decreased [*Bain et al.*, 1998]. Finally, $^{87}Sr/^{86}Sr$, [Ca]/[Sr], and [Ba]/[Sr] ratios were used to separate streamflow into soil water, shallow groundwater and deep groundwater at a larger catchment (9.4 km^2) in northern Sweden. Separation was possible because the differential weathering susceptibility of minerals in the substrate was found to impart distinct ratios to different flow paths [*Land et al.*, 2000].

[6] In this study, we examine the ability of Sr isotopes to trace water flow paths within a small forested watershed. At our study site there is a strong contrast in the $^{87}Sr/^{86}Sr$ ratio of Sr derived from atmospheric inputs ($\sim$0.710) versus silicate mineral weathering (0.730 to 0.736; *Blum et al.*, 2002) which leads to a gradient in $^{87}Sr/^{86}Sr$ ratios and allows us to trace the flow path that water takes to the stream channel. Channel interception of throughfall should have the lowest $^{87}Sr/^{86}Sr$ ratio (closest to the atmospheric end-member), followed by shallow sub-surface flow (water that travels predominantly through soils). Groundwater flow (which generates base flow) has the highest $^{87}Sr/^{86}Sr$ ratios, closest to the weathering end-member. Ratios of Sr concentration to other solutes that display a similar geochemical behavior (i.e., Ca and Ba, which are located above and below Sr on the periodic table), are used as an additional constraint on end-member compositions. To test the use of $^{87}Sr/^{86}Sr$, [Ca]/[Sr] and [Ba]/[Sr] as tracers of hydrologic flow paths we analyzed stream water collected during two rain events and one snowmelt event. These results were compared with $\delta^{18}O$ values to explore whether they provide distinct hydrologic information.

[7] A companion study (Hogan et al., manuscript in preparation, 2003) examined the variability of thirteen major and trace elements. Four distinct types of solutes were recognized. Type I solutes (K, Rb, B) are elevated in throughfall because they are readily leached from foliage. Type II solutes showed high concentrations in soil water because they are released preferentially through the microbial decay of organic matter (NO_3) or chemical weathering in soils (Ba). Type III solutes (Na, Mg, Si) exhibited the highest concentrations in groundwater due to supply from mineral weathering. For type IV solutes, concentrations are roughly the same in all end-member waters because inputs are largely from atmospheric deposition (Cl, SO_4), or because inputs from chemical weathering appear to be balanced by biological cycling within this catchment (Ca, Sr, Li). Each solute type exhibited distinct variation during the course of a storm event. In order to explain the observed variation three end-member waters are needed: (1) groundwater (base flow); (2) shallow subsurface flow of soil water, and (3) direct channel interception of throughfall.

2. Mixing Models

[8] With proper selection of end-member compositions and a simple geochemical mixing model, changes in $^{87}Sr/^{86}Sr$ ratios and $\delta^{18}O$ values of stream water can be used to estimate the percentage of water from various hydrologic flow paths (see *Albarede* [1995] for a general discussion of mixing equations). For oxygen isotopes, the two-component mixing model for new and old water can be expressed as:

$$\delta^{18}O_{mix} = (1 - x)\delta^{18}O_{old} + (x)\delta^{18}O_{new} \quad (1)$$

where old refers to pre-event water, new refers to precipitation, mix refers to the mixture in the stream water, and the variable x is the fraction of new water in the mixture. Similarly, one can look at the mixing relationships of $^{87}Sr/^{86}Sr$ ratios. As a solute, variations in the Sr concentration also need to be taken into account. To do this each end-member water is weighted by the fraction of Sr from that end-member in the resulting mixture. For Sr isotopes a three-component mixing model for stream water can be expressed as:

$$\left(^{87}Sr/^{total}Sr\right)_{mix} = y\frac{[Sr]_{gw}}{[Sr]_{mix}}\left(^{87}Sr/^{total}Sr\right)_{gw} + (1 - y - x)\frac{[Sr]_{sw}}{[Sr]_{mix}}\left(^{87}Sr/^{total}Sr\right)_{sw} + x\frac{[Sr]_{thf}}{[Sr]_{mix}}\left(^{87}Sr/^{total}Sr\right)_{thf} \quad (2)$$

where: *gw* represents the deep groundwater flow path (with base flow used for an end-member composition), *sw* is shallow subsurface flow (with soil water used for an end-member composition), *thf* is channel interception of throughfall and *mix* refers to the mixture in the stream water. This equation has two unknown variables, y which represents the fraction of groundwater flow in the stream mixture, and x which represents the fraction of throughfall. In order to solve this equation we assume that the fraction

of new water (x in equation 1) is the same as the fraction of throughfall (x in equation 2). In doing this we have made the assumption that new water reaches the stream only by channel interception of throughfall. This is consistent with several studies done in other humid headwater catchments where most or all of the new water can be accounted for by channel interception and saturation overland flow [e.g., *Pearce et al.*, 1986; *Sklash et al.*, 1986; *Dewalle and Sharpe*, 1988; *McDonnell et al.*, 1991].

[9] In addition to the mixing of waters from different flow paths, variation in the $^{87}Sr/^{86}Sr$ ratio of stream waters could result from chemical reactions that release Sr with a distinct $^{87}Sr/^{86}Sr$ ratio. The two most common types of reactions are mineral dissolution and cation exchange. Mineral dissolution is unlikely to affect the $^{87}Sr/^{86}Sr$ ratio of stream water because of the slow reaction rates and the short residence time of water in the stream channel of a headwater catchment. Cation exchange reactions, which occur at much faster rates, could be significant and their effect needs to be considered. Even though the stream sediments at the study site range from sand to gravel size, and thus have low surface area, tracer injection experiments have shown that the transport of Sr and Ca can be appreciably modified by sorption onto streambed sediments [*Bencala*, 1984; *Bencala et al.*, 1984; *Hall et al.*, 2001]. Two factors should minimize the effects of cation exchange reactions on this study. First, presumably there is an equilibrium between dissolved Sr in stream water and Sr sorbed on stream sediment. Because the Sr concentration does not change significantly during the course of a storm event and has approximately the same concentration in all end-member waters, there is no chemical gradient to drive Sr onto or off of exchange sites. Second, uptake of Ca by stream sediments appears to depend upon stream pH; in an unbuffered stream with a low pH, such as this study site, there is minimal uptake. This is most likely due to a greater number of negatively charged exchange sites on mineral surfaces at higher pH [*Hall et al.*, 2001]. Finally we note that the $^{87}Sr/^{86}Sr$ ratio for exchangeable Sr within the channel should reflect the average composition of stream water. Because of this, any exchange reactions that do occur would buffer changes in stream water $^{87}Sr/^{86}Sr$ ratios, rather than enhance them. Thus any changes in stream $^{87}Sr/^{86}Sr$ could be considered minimum changes for water inputs, and the percentage of flow calculated using Sr isotope variations for shallow subsurface flow and channel interception of throughfall would also represent minimum values.

3. Site Description

[10] This study was conducted at watershed 1 (W1) of the Hubbard Brook Experimental Forest (HBEF) (Figure 1). HBEF is located within the White Mountain National Forest near West Thorton, New Hampshire (43°56′N, 71°45′W). A detailed description of HBEF is given by *Likens and Bormann* [1995], and thus only the most pertinent information is given here. W1 is a perennial first order catchment 11.8 ha in area. The U.S. Forest Service maintains a 90°V notch weir and a rain gauge, which continuously record stream discharge and precipitation. Precipitation averages 1395 mm/yr and is evenly distributed throughout the year. Of this, 25–33% falls as snow. About 50% of annual stream discharge occurs as a result of snowmelt during the months

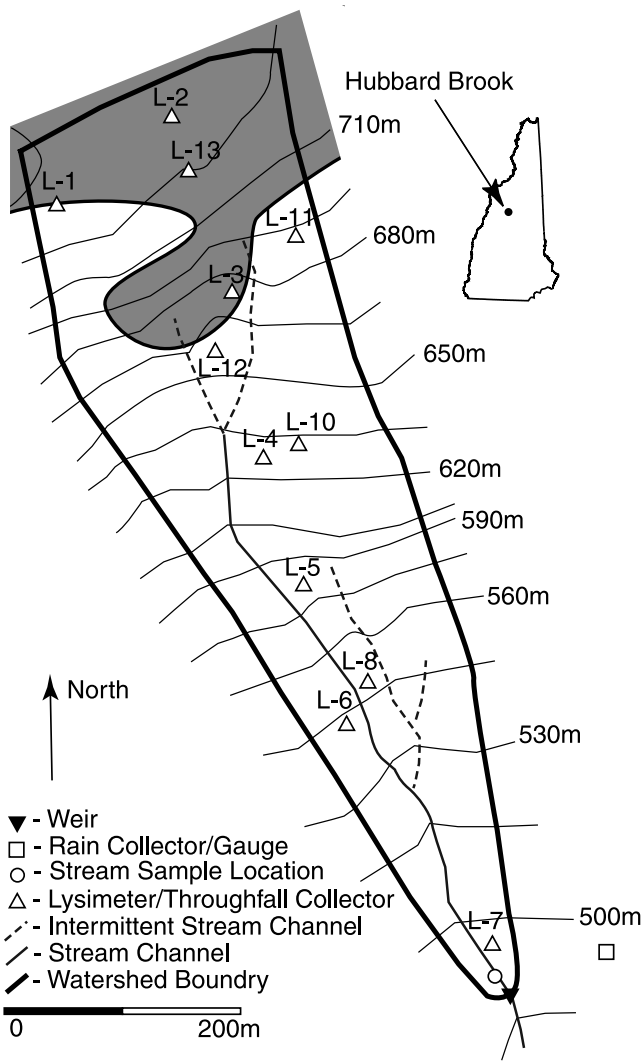

Figure 1. Map of watershed 1 in the Hubbard Brook Experimental Forest detailing sample collection sites. Shaded area represents area of spruce/fir forest in the upper part of the watershed.

of March, April, and May [*Federer et al.*, 1990]. During the summer months stream discharge is typically very low, and most water is lost through evapotranspiration. Evapotranspiration remains relatively constant from year to year at ~500 mm/yr, even as total precipitation changes considerably [*Likens and Bormann*, 1995].

[11] The bedrock of the watershed is composed of the upper member of the Silurian Rangeley formation, a rusty-weathering pelitic schist containing calc-silicate pods. The Rangeley is locally intruded by granite, pegmatite and diabase [*Barton*, 1997]. The bedrock has very low permeability and thus there is minimal loss of water from the catchment by deep seepage [*Likens and Bormann*, 1995]. Mantling the bedrock is a layer of glacial till, ~1 m thick, made up predominantly of clasts of the Rangeley formation and the Kinsman granodiorite. Well-drained spodosol soils are developed on the glacial till. Soils consist of a 6–9 cm organic layer (Oa horizon) underlain by 40–60 cm of mineral soil (A + B horizons) [*Johnson et al.*, 2000]. Soil thickness, however, is highly variable with thin soils at

higher elevation and along the ridge tops and thicker soils at the lower elevations [*Likens and Bormann*, 1995]. Because the soils are quite porous most of the precipitation infiltrates the soil quickly with little overland flow [*Pierce*, 1967]. A northern hardwood forest, composed of sugar maple (*Acer sacchararum*), America beech (*Fagus grandifolia*), and yellow birch (*Betula alleghaniensis*), covers 80–90% of the watershed. Conifers, dominantly red spruce (*Picea rubens*) and Balsam fir (*Abies balsamea*), make up the remaining 10–20% and are common along the ridge tops at higher elevations (Figure 1) [*Likens and Bormann*, 1995].

4. Methods

[12] In order to assess spatial and temporal heterogeneity in $^{87}Sr/^{86}Sr$, [Ca]/[Sr] and [Ba]/[Sr] ratios we sampled soil water and throughfall at 12 sites in the watershed (Figure 1). Soil water was collected from zero tension lysimeters. Three sites (L-6, L-7, L-13) along the length of the watershed were selected for analysis of soil water variability both seasonally and with depth in the soil profile. Soil water at these sites was analyzed from Oa, Bh and Bs horizons during all four seasons. For the other 9 lysimeter sites, soil water was analyzed only from the Bs horizon in March 1999. Throughfall was collected at each of the 12 lysimeter sites during the month of July in 1999 using 25 cm diameter HDPE plastic funnels with a plastic mesh filter at the base to filter coarse particulates. Funnels were connected to narrow-mouth HDPE bottles using plastic tubing; the plastic tubing was twisted into a loop in order to prevent sample evaporation and samples were collected within two days of precipitation events.

[13] In order to determine the variability of stream water $^{87}Sr/^{86}Sr$, [Ca]/[Sr], [Ba]/[Sr] and $\delta^{18}O$ during storm events we sampled both precipitation and stream water approximately hourly. Samples were collected in acid-cleaned HDPE bottles for elemental and Sr isotope analysis and glass vials with polyseal caps for O isotope analysis. Precipitation was collected using a HDPE plastic funnel (25 cm diameter) connected to a 125 mL FEP separatory funnel to allow for sampling during the storm events. The precipitation collector was located in the same clearing as the rain gauge (see Figure 1).

[14] We analyzed samples for Ca, Sr and Ba concentrations, after spiking with a 10 ppb indium internal standard, using a Finnigan Element inductively coupled plasma mass spectrometer. Calibration curves had r^2 values greater than 0.9999. Analysis of NIST SRM 1643d (Trace Elements in Water) agreed within 5% of reported values. Concentrations are reported in this paper in units of ppb (ng/g), and elemental ratios are reported as mass ratios. The United States Geological Survey Menlo Park (November 1997 storm) and the University of Arizona Isotope Geochemistry Laboratory (September 1998 storm) performed the oxygen isotope analyses.

[15] For Sr isotope analysis, samples of ~50 mL of water, containing between 200 and 300 ng of Sr, were evaporated in 15 mL Teflon beakers. Samples were then redissolved in 1 mL of 3M distilled HNO_3 and the Sr separated for isotopic analysis using Sr Specific Resin (Eichrom). Aliquots containing 75 ng of Sr were evaporated in 7 mL Teflon beakers, then redissolved in 1 μL of 0.3 M H_3PO_4 and loaded onto single tungsten filaments with Ta_2O_5 powder. The Sr isotopic compositions were determined on a Finnigan MAT 262 multicollector thermal ionization mass spectrometer operating in static mode. All $^{87}Sr/^{86}Sr$ values were corrected for mass fractionation to $^{86}Sr/^{88}Sr = 0.1194$ and have a precision of at least ± 0.000015 (2se). Total analytical blanks were <40 pg and are thus negligible. Replicate analysis of NIST SRM-987 during the period of analysis yielded a $^{87}Sr/^{86}Sr$ value of 0.710262 ± 0.000013 (n = 32, 2se).

Table 1. Oxygen Isotope End-Member Compositions

	Old Water			New Water		
Event	n	$\delta^{18}O_{str}$	1σ	n	$\delta^{18}O_{ppt}$	1σ
November 1997	4	−9.78	0.03	4	−14.5	0.76
September 1998	3	−9.8	0	7	−5.6	2.65

5. Results and Discussion

5.1. Oxygen Isotopic Composition of "New" and "Old" Waters

[16] In order to trace hydrologic flow paths and perform a hydrograph separation using a stream water mixing model (equations 1 and 2), one must be able to select appropriate end-members compositions for each storm event and understand their variability. O isotopes end-members values were determined for ''old water'' and ''new water'' following established methods. The old water end-member was assumed to be the average $\delta^{18}O$ value of stream water prior to the start of each event, whereas new water was based on a weighted average of the $\delta^{18}O$ value of precipitation (Table 1). Pre-event water for both the November 1997 and the September 1998 storm events had an average isotopic composition of −9.8‰. The $\delta^{18}O$ value for new water from the November 1997 storm event was −14.5‰, and was relatively constant throughout the storm. A brief period of rain at the end of the storm event did have a distinct isotopic composition (~−7.7‰) but was not included as it occurred on the falling limb of the hydrograph and was not volumetrically significant. $\delta^{18}O$ values for precipitation during the September 1998 storm were more variable. The early part of the storm averaged ~−5‰. This was followed by a period of heavy rain that resulted in the greatest change in stream discharge. The $\delta^{18}O$ values for this period showed a distinct rainout pattern, with rain initially having a heavy isotopic composition (−4.1‰), then becoming increasingly lighter through the storm event, ending with a value of −9.3‰. The weighted average composition was −5.6‰. This variability in the precipitation will result in an overestimate of the new water contribution to streamflow during the early stages of the storm event when the actual $\delta^{18}O$ value for precipitation was ~1‰ lighter, and an underestimate of the new water contribution during the latter stages because precipitation was ~1‰ heavier than the $\delta^{18}O$ value used for the precipitation end-member in the hydrograph separations.

5.2. [Ca]/[Sr], [Ba]/[Sr], and $^{87}Sr/^{86}Sr$ Ratios of End-Member Waters

[17] For hydrograph separation using Sr isotopes, the Sr concentration and $^{87}Sr/^{86}Sr$ ratio must be defined for the three water end-members: groundwater flow, shallow sub-

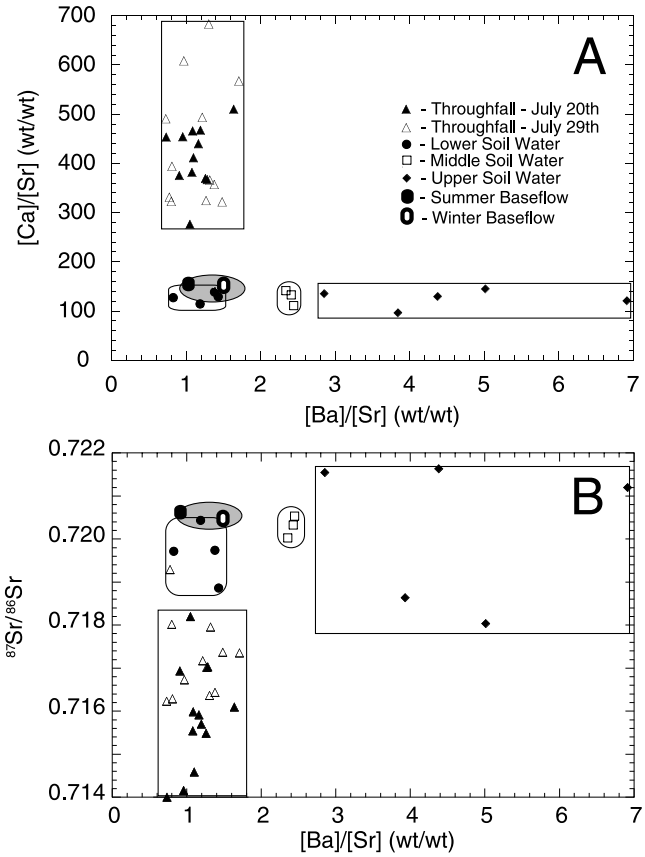

Figure 2. End-member discrimination plots using (a) [Ca]/[Sr]-[Ba]/[Sr] ratios and (b) $^{87}Sr/^{86}Sr$-[Ba]/[Sr] ratios. Boxed areas highlight throughfall and soil water end-members. Note that soil water plots in three distinct elevational fields due to a systematic variation in [Ba]/[Sr] ratios. Shaded oval represents the field for all stream water samples in this study, with the summer and winter base flow values highlighted.

surface flow and channel interception. Selecting a composition for the groundwater flow end-member is straightforward; base flow prior to the start of the storm event provides an average composition of groundwater flow to the stream channel. Selection of the shallow subsurface flow and channel interception of throughfall is more complex because: (1) there is considerable spatial variability within the watershed and (2) soil water and throughfall samples were collected at times other than during the storm events studied. In order to understand the observed heterogeneity and to better constrain our end-member compositions we first need to examine the end-member discrimination plots using [Ca]/[Sr], [Ba]/[Sr] and $^{87}Sr/^{86}Sr$ ratios (Figure 2).

5.2.1. Base Flow-Groundwater Flow

[18] The $^{87}Sr/^{86}Sr$ ratio of stream base flow at the start of the November 1997 and September 1998 storm events was 0.72049 and 0.72047 respectively, and the [Ba]/[Sr] ratio was ~1.0. In contrast, the $^{87}Sr/^{86}Sr$ ratio of base flow for the March 1999 snowmelt event was 0.72034 and the [Ba]/[Sr] ratio was 1.5 (Figure 2b), substantially different from the summer/fall storm events. This difference is probably due to seasonal variation in the chemical composition of base flow related to changes in water residence time. Longer residence times during the summer months allow for a greater influence from chemical weathering along deeper water flow paths and result in a higher $^{87}Sr/^{86}Sr$ ratio and lower [Ba]/[Sr] ratio for base flow. During the winter months shorter residence times result in lower $^{87}Sr/^{86}Sr$ ratios and higher [Ba]/[Sr] ratios, closer to soil water compositions. In contrast, the [Ca]/[Sr] ratio of base flow is relatively consistent with a value of 135–140. The November 1997 storm event does have an elevated [Ca]/[Sr] ratio (160); this may be due to leaching of recently fallen leaves in the stream during the seasonal canopy loss.

5.2.2. Throughfall-Channel Interception

[19] Throughfall from the 20 July 1999 collection had an average Sr concentration of 2.3 ± 1.0 (1σ) ppb with an $^{87}Sr/^{86}Sr$ ratio of 0.7158 ± 0.0012 (1σ), whereas the 29 July 1999 collection had an average Sr concentration of 3.1 ± 2.3 (1σ) ppb with an $^{87}Sr/^{86}Sr$ ratio of 0.7172 ± 0.0009 (1σ). Even though the $^{87}Sr/^{86}Sr$ ratio is distinct for the two throughfall collections, there is no significant difference in the [Ba]/[Sr] ratio (1.12 ± 0.22 (1σ) versus 1.14 ± 0.32 (1σ)) or [Ca]/[Sr] ratio (414 ± 64 (1σ) versus 438 ± 127 (1σ)). The [Ca]/[Sr], [Ba]/[Sr] and $^{87}Sr/^{86}Sr$ ratios are relatively uniform throughout the watershed (Figure 2).

[20] Throughfall samples consistently have the highest [Ca]/[Sr], the lowest $^{87}Sr/^{86}Sr$ ratios, and have among the lowest [Ba]/[Sr] ratios (Figure 2) of waters samples in the watershed. Interestingly, the 20 July throughfall collection is distinctly lower in $^{87}Sr/^{86}Sr$ ratios than the 29 July collection. This may be related to the fact that there were 8 dry days prior to the rain event on 20 July, whereas there were only 4 dry days between rainfall events for the 29 July collection, thus allowing for greater atmospheric deposition to the foliage and $^{87}Sr/^{86}Sr$ ratios closer to the atmospheric value of 0.7106 [*Bailey et al.*, 1996]. Likewise, we observe a slight shift in the [Ca]/[Sr] ratio toward the atmospheric values of ~100; [*Bailey et al.*, 1996]. This change is mainly attributed to a few 29 July samples with significantly elevated [Ca]/[Sr] ratios and likewise results in significantly higher variance for the 29 July sampling. There is no change for the [Ba]/[Sr] ratio of throughfall; this is to be expected because the throughfall ratio is essentially the same as atmospheric value of ~1.1 [*Simonetti et al.*, 2000]. The [Ca]/[Sr] ratio for throughfall is consistently higher than the corresponding soil water, whereas the [Ba]/[Sr] ratio is consistently lower in the upper and middle portions of the watershed, but is equal to lower elevation soil water values. Throughfall values are consistent with values for tree foliage at HBEF which have [Ca]/[Sr] ratios that are higher than the corresponding soil solutions [*Blum et al.*, 2002] and lower or equal to soil water [Ba]/[Sr] ratios (Blum, unpublished data).

[21] As throughfall does not show any systematic pattern of spatial variation, we based the $^{87}Sr/^{86}Sr$ ratio and concentration of this end-member on an average of all throughfall samples (Table 2). For the November 1997 storm event we used the same $^{87}Sr/^{86}Sr$ ratio but reduced the Sr concentration by one third to 1 ppb. The decrease in throughfall concentration is a result of the seasonal loss of canopy foliage, which occurs from mid-October to early November. The one-third reduction was selected because the increase in potassium concentration (a solute closely

Table 2. Strontium Isotope End-Member Compositions

Event	n	$^{87}Sr/^{86}Sr_{gw}$	1σ	$[Sr]_{gw}$
		Groundwater		
November 1997	4	0.72049	0.00001	5.6
September 1998	5	0.72047	0.00003	6.1
March 1999	1	0.72034	–	7.2
		Soil Water		
November 1997	7	0.72007	0.00074	6
September 1998	7	0.72007	0.00074	6
March 1999	7	0.72007	0.00074	5.1
		New Water/Throughfall		
November 1997	24	0.7165	0.0013	1
September 1998	24	0.7165	0.0013	2.7

linked with throughfall) of stream water during the November 1997 storm was 1/3 the value observed for the September 1998 event (Hogan et al., manuscript in preparation, 2003). For the snowmelt event, because there is no canopy present, we assume that the throughfall end-member is simply the same as precipitation. Because the Sr concentration of precipitation for this area is approximately one order of magnitude less than for stream water [*Bailey et al.*, 1996] this end-member has little effect on the Sr isotopic composition of stream water and is therefore not included in the hydrograph separation for this storm event.

5.2.3. Soil Water-Subsurface Flow

[22] Analyses of soil water from the three intensively studied sites showed Sr concentrations to vary from 4 to 14 ppb and [Ca]/[Sr] ratios to vary from 140 to 230. The highest concentrations and ratios occurred during the summer and fall, and variations were most pronounced for soil waters from the Oa horizon (Figures 3a and 3b). During the winter and spring [Sr] and [Ca]/[Sr] tended to be lower and more uniform with depth in the soil profile. In contrast, $^{87}Sr/^{86}Sr$ and [Ba]/[Sr] ratios (Figures 3c and 3d) exhibited only minor variation with depth in the soil profile or through the changing seasons, but did display substantial site-to-site variability.

[23] The low seasonal variability below the Oa horizon (Figure 3) allows us to use a single sampling of soil water (March 1999) from throughout the watershed to constrain the soil water end-member. Results from the March 1999 sampling of lysimeter water from the Bs horizon of all 12 sites yielded an average Sr concentration of 3.9 ppb ±

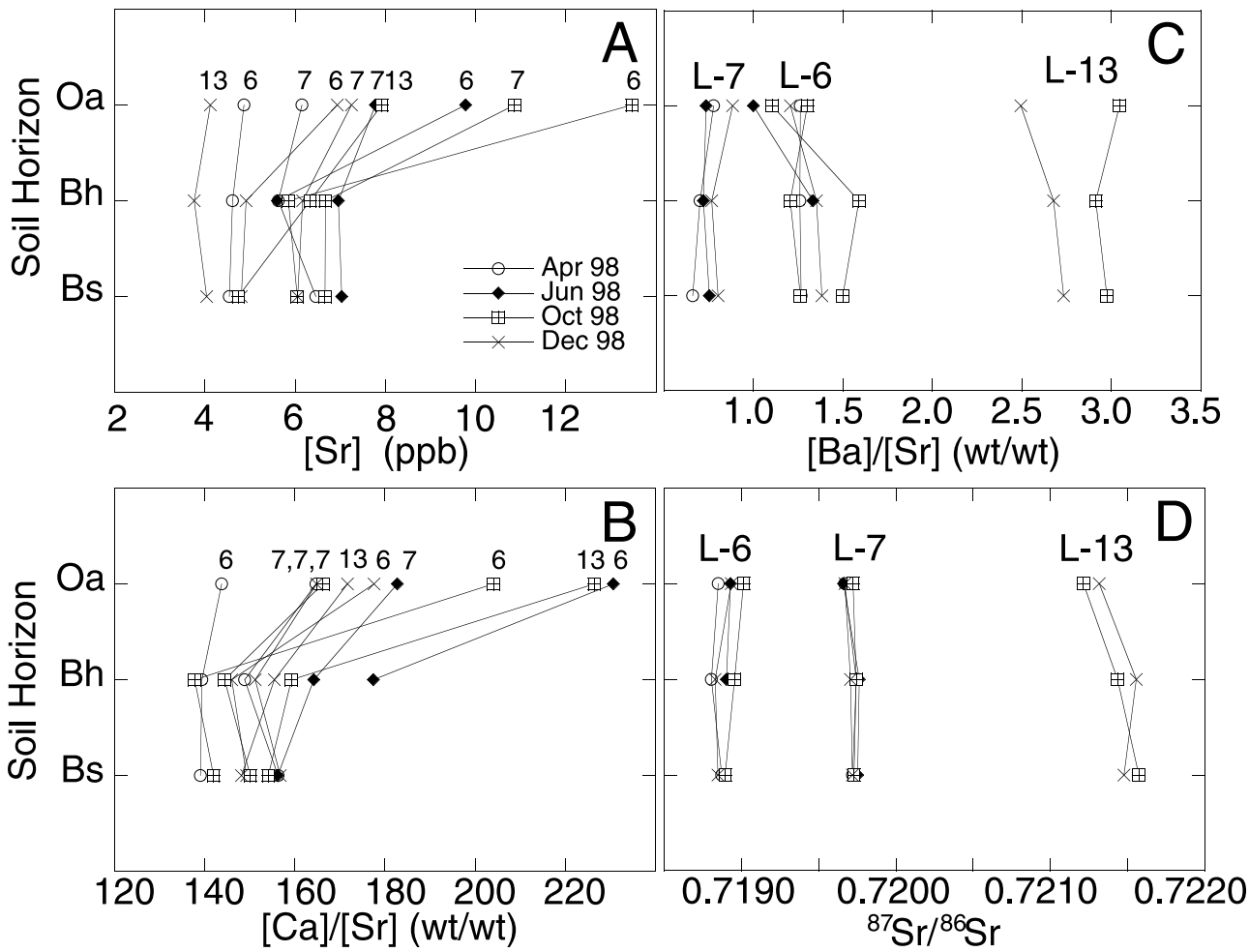

Figure 3. Vertical soil waters profiles for the intensively studied lysimeters (L-6, L-7, and L-13). (a) Sr concentrations and (b) [Ca]/[Sr] ratios exhibit elevated values during the summer and fall for all three lysimeters, especially for the Oa horizon. In contrast, both (c) [Ba]/[Sr] ratios and (d) $^{87}Sr/^{86}Sr$ ratios have little variability within the profile or through the year. Site to site variability, however, is quite high.

1.8 (1σ) and $^{87}Sr/^{86}Sr$ ratio of 0.720 ± 0.001 (1σ). When soil water data are plotted on discrimination diagrams using [Ca]/[Sr], [Ba]/[Sr] and $^{87}Sr/^{86}Sr$ ratios, three distinct soil waters can be recognized (Figure 2). Soil water from lysimeters in the lower portion of the watershed (L-5, 6, 7, 8) have the lowest $^{87}Sr/^{86}Sr$ and [Ba]/[Sr] ratios (0.7197 ± 0.0006 and 1.2 ± 0.3 respectively). The middle part of the watershed (L-4, 10, 12) has slightly higher $^{87}Sr/^{86}Sr$ and [Ba]/[Sr] ratios (0.7203 ± 0.0003 and 2.41 ± 0.05 respectively). Finally, soil water from the upper part of the watershed (that area above 665 m) has both the highest and lowest $^{87}Sr/^{86}Sr$ ratio observed for soil water (0.7202 ± 0.0017). In contrast, [Ba]/[Sr] ratios in the upper part of the watershed are consistently higher (4.6 ± 1.5) than those of the lower and middle parts of the watershed. In contrast to [Ba]/[Sr] and $^{87}Sr/^{86}Sr$, [Ca]/[Sr] ratios have a very narrow range, 126 ± 13 (1σ), that does not correlate with elevation (Figure 2a).

[24] The results for soil water compositions raise two important questions for this study. First, why are there significant changes in [Sr] and [Ca]/[Sr] ratios, both seasonally and with depth, whereas no variation was observed for [Ba]/[Sr] and $^{87}Sr/^{86}Sr$ ratios (Figure 3). The increase in Sr concentration during the summer months, notably in the Oa horizon, is due in part to increased evapotransparition (ET). Chloride concentrations for lysimeter waters exhibit a ~50% increase in summer (9.5 ppm in April to 14.6 ppm in October; Driscoll, unpublished data), at all depths in the soil profiles. Sr exhibits a similar percentage increase for soil water in the B horizons, however the increase in the Oa horizon is far greater than can be explained by ET alone. An increase in the [Ca]/[Sr] ratio for the Oa horizon also indicates that there is an additional Sr source (Figure 3b). This additional source could be Sr released through decay or leaching of leaf litter, a process that would increase Sr concentration but have no effect on Cl concentration. The high [Ca]/[Sr] ratio of throughfall (Figure 2a) and foliage [*Blum et al.*, 2000, 2002] compared to soil water is consistent with this mechanism.

[25] One might be surprised that the $^{87}Sr/^{86}Sr$ ratio of soil water does not increase with depth in the soil profile from the addition of radiogenic Sr released through chemical weathering. However, it is important to keep in mind that the soil water in this study is collected using zero-tension lysimeters which intercept mobile soil water, most likely flowing quickly along macropores during storm events. Because of this, there is little time for soil water to gain Sr released through weathering. A similar sampling effect was shown for the oxygen isotopic composition of soil water collected using wick samplers, suction lysimeters and soil cores, each of which method was found to be distinct, with wick samplers collecting mobile event water almost exclusively [*Landon et al.*, 1999]. Zero-tension lysimeters probably also sample this quick flowing fraction of the soil water, which is the fraction most likely to contribute to streamflow during a storm event.

[26] The second question is what explains the observed spatial variability for [Ba]/[Sr] and $^{87}Sr/^{86}Sr$ ratios, especially as it relates to elevation within the watershed. The reason for the elevational variability in [Ba]/[Sr] of soil waters is not entirely clear, but is also reflected in the [Ba]/[Sr] of the soil exchange complex (Blum, unpublished data). We note that this variation corresponds to vegetation changes, notably the spruce-fir zone occurs exclusively in the upper part of the watershed. We suggest that the vegetation changes affect the composition of soil water by changing the chemical weathering regime. Coniferous trees produce higher levels of organic acids in soil solutions, which could result in a more intense chemical weathering environment. K-rich minerals in the soil parent material at HBEF, such as K-feldspar and muscovite, are more resistant to weathering and have higher [Ba]/[Sr] ratios than Ca-rich minerals such as plagioclase and apatite. Chemical analyses of bulk soils indicate that K-rich minerals are weathered to a greater extent at higher compared to lower elevations in W-1 [*Nezat et al.*, unpublished data]. More rapid weathering of K-rich minerals has also been linked to high [Ba]/[Sr] ratios in soil waters from other catchments [*Land and Ohlander*, 1997]. The K-rich minerals also have high [Rb]/[Sr] ratios and thus would be expected to have somewhat higher $^{87}Sr/^{86}Sr$ ratios. However, there is no simple correlation between [Ba]/[Sr] and $^{87}Sr/^{86}Sr$ in soil waters suggesting that this may not be the only mechanism controlling these ratios. Some minor heterogeneity in till composition may also contribute to the full explanation of the variations in both [Ba]/[Sr] and $^{87}Sr/^{86}Sr$ ratios for soil water.

[27] The $^{87}Sr/^{86}Sr$ ratio of the shallow subsurface flow path is taken to be the average $^{87}Sr/^{86}Sr$ ratio of soil water from lysimeters located in the lower and middle portions of the watershed (Table 2). These lysimeters were selected because they are located relatively close to the stream channel representing an area that could potentially contribute shallow subsurface flow during a storm event. In contrast, lysimters from the upper part of the watershed are some distance from the stream channel making it unlikely that soil water collected here will contribute to streamflow on the timescale of a storm event, and furthermore if they did the distance traveled would likely result in changes in the end-member composition. We note that if the soil water end-member was based on an average all lysimeter waters the $^{87}Sr/^{86}Sr$ ratio would barely change, however given the heterogeneity of the upper soil water there would be significantly greater uncertainty in its value. Because the $^{87}Sr/^{86}Sr$ ratio of lysimeter water does not change appreciably with depth or seasonally the same value can be used for both storm events and the snowmelt event. The Sr concentration of soil water does however change both with depth and season. Because of this we based the Sr concentration of the soil water end-member on the average Sr concentration from the Bs horizon because, as the thickest and deepest horizon in the soil profile, it is the most likely to contribute to storm flow. The Sr concentration of soil water for the snowmelt event was based on the average Sr concentration for the Bs horizon of all twelve sites sampled in March of 1999 (5.3 ppb). For the November 1997 and September 1998 storm events the Sr concentration was increased to 6 ppb based on the average Sr concentrations in the Bs horizon from the June and October samples for the three lysimeters studied in detail (Figure 3a).

5.3. Storm Events

[28] We sampled three storm events. A fall rain event, sampled on 1–2 November 1997 (Figure 4), totaled 26.6 mm of rain, most of which (~24 mm) fell during a

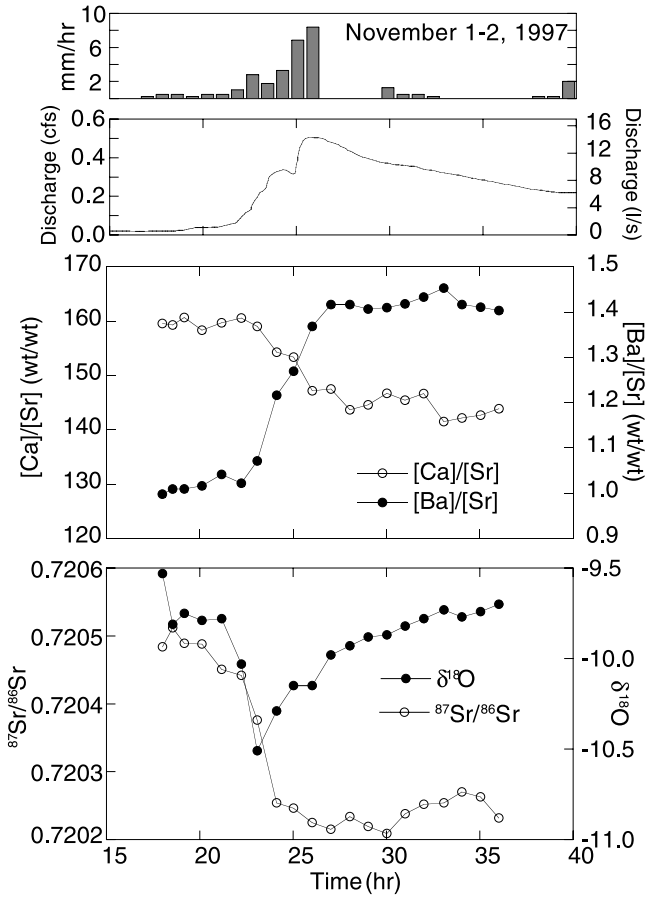

Figure 4. Hourly precipitation rate, stream discharge, solute ratio, and isotope ratio measurements for the fall storm event sampled on 1–2 November 1997. Time is in hours after midnight, 1 November 1997.

six hour period. A late summer rain event, sampled on 15–16 September 1998 (Figure 5), totaled 38.1 mm of rain, most of which (~25 mm) fell during a two hour period. Finally, a rain on snow event (Figure 6) was sampled on 22 March 1999. This event can be characterized by two distinct periods, a 12 hour period when 33 mm of rain fell onto a ripe snowpack (i.e., one that is close to 0°C and capable of producing snowmelt), followed by a warm sunny day with additional melting of the snowpack.

[29] During each storm event there was a shift in stream water to lower $^{87}Sr/^{86}Sr$ ratios, with the greatest change occurring near peak discharge. There are some important distinctions between the three events. Comparing the two rain events, the change in the $^{87}Sr/^{86}Sr$ ratio of stream water was greater for the November 1997 storm (~0.72050 to ~0.72020) than for the September 1998 storm (~0.72050 to ~0.72035). In addition, the $^{87}Sr/^{86}Sr$ ratio of stream water returned to higher $^{87}Sr/^{86}Sr$ ratios more rapidly during the September 1998 storm than the November 1997 storm. When comparing the rain on snow event to the two rain events there are three important differences. First, the $^{87}Sr/^{86}Sr$ ratio of stream water at the start of the snowmelt event was much lower (0.72035) than for the two rain events (0.72050). Second, unlike the rain events, the $^{87}Sr/^{86}Sr$ ratio of steam water on the falling limbs of the hydrograph rose to values higher than that of the pre-event stream water. Lastly, the period of snowmelt at the end of the event resulted in a leveling off of the stream hydrograph and a slight decrease in the $^{87}Sr/^{86}Sr$ ratio of the stream water.

[30] Results of $\delta^{18}O$ analysis for the two rain events showed a shift in stream $\delta^{18}O$ toward the value of rainfall specific to each of the rain events (November 1997: −14.5‰ ± 0.8; Sept. 1998: −5.6‰ ± 2.7). The greatest change in the $\delta^{18}O$ value of stream water occurred during the period of greatest rainfall, typically before the period of highest stream discharge. In contrast to $^{87}Sr/^{86}Sr$ ratios, $\delta^{18}O$ values quickly returned to values similar to the start of the storm even as stream discharge remained high. The $\delta^{18}O$ values were not measured for the snowmelt event. Previous studies have suggested that $\delta^{18}O$ heterogeneity within the snowpack makes constraining the new water end-member difficult using oxygen isotopes [*Hooper and Shoemaker*, 1986].

[31] The [Ca]/[Sr] and [Ba]/[Sr] ratios of stream water both also respond to storm events. The [Ca]/[Sr] ratio exhibits a varied response, from a slight decrease during the November 1997 event (160–145; Figure 4), elevated ratios during periods of rain for the September 1998 (130–155, Figure 5), and finally no change during the March 1999 event (Figure 6). The only end-member water

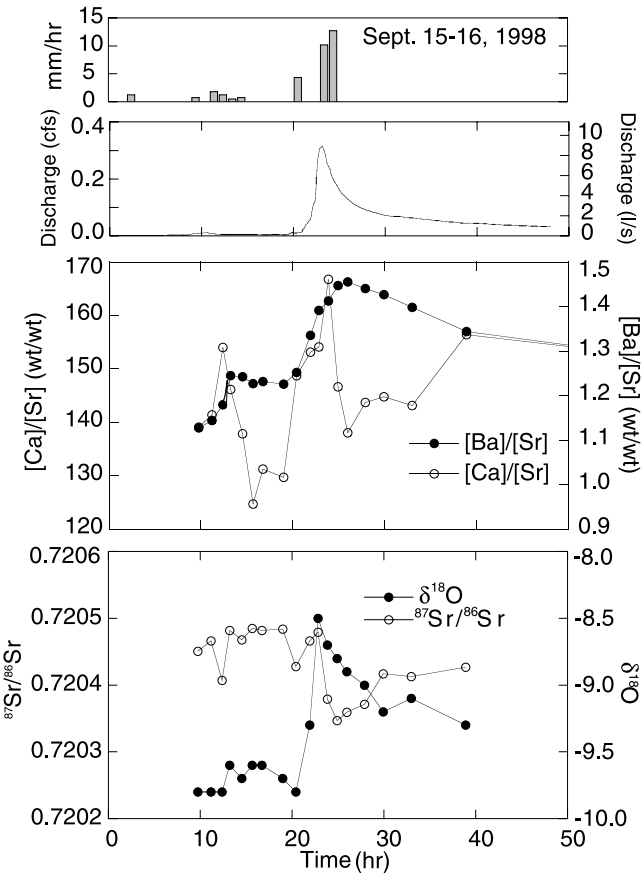

Figure 5. Hourly precipitation rate, stream discharge, solute ratio, and isotope ratio measurements for the late summer storm event sampled on 15–16 September 1998. Time is in hours after midnight, 15 September 1998.

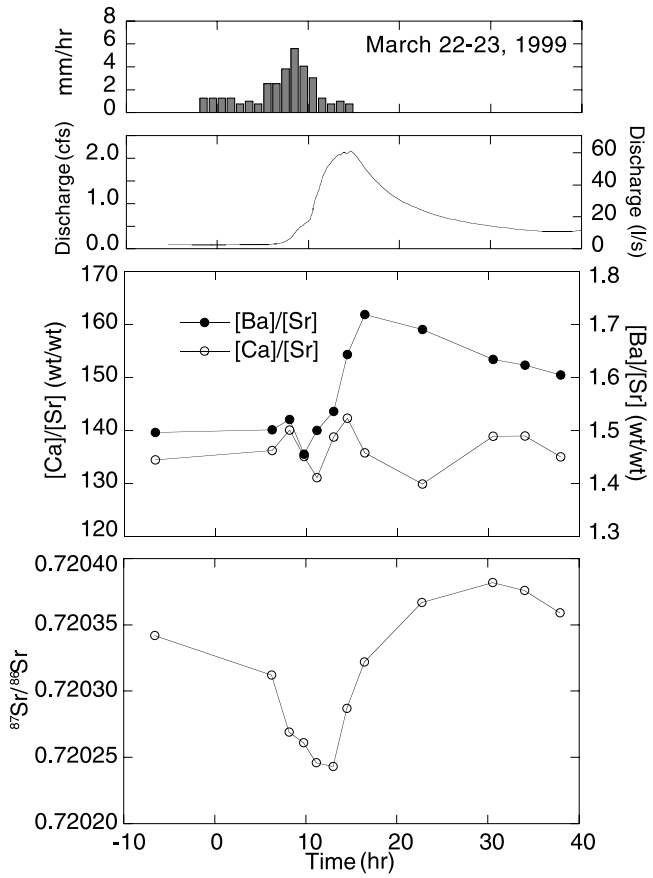

Figure 6. Hourly precipitation rate, stream discharge, solute ratio, and isotope ratio measurements for the snowmelt event sampled on 22–23 March 1999. Time is in hours after midnight, 23 March 1999.

that exhibits a distinct [Ca]/[Sr] ratio is throughfall (Figure 2a). Because of this, one would expect the [Ca]/[Sr] ratio of stream water to change only with throughfall inputs. For the September 1998 storm event this is exactly what is observed, with the [Ca]/[Sr] ratio of stream water increasing during both periods of rain (Figure 5). However, during the other events different patterns of change are observed. For the March 1999 snowmelt event there is essentially no change in the [Ca]/[Sr] ratio (Figure 6). As this event occurs during the winter, with leaves off, throughfall will not affect the [Ca]/[Sr] ratio and stream water therefore would not be expected to change. Finally, during the November 1997 storm event we see a decreasing [Ca]/[Sr] ratio for stream water (Figure 4). As was mentioned earlier, the [Ca]/[Sr] ratio at the start of this event is elevated (160), possibly as a result of in-stream leaching of recently fallen leaves. This initially elevated [Ca]/[Sr] ratio probably obscures any throughfall signal during the initial stages of the storm event. Latter in the event as the stream discharge increased, the [Ca]/[Sr] ratio also decreased; this is consistent with contributions from groundwater and soil water (which have lower [Ca]/[Sr] ratios), reducing the relative importance of contributions from throughfall and in-stream leaching.

[32] In contrast to [Ca]/[Sr], [Ba]/[Sr] ratios consistently show increasing ratios with increasing flow, a pattern of change that is similar to that observed for Sr isotope ratios. [Ba]/[Sr] varied between 1.0 and 1.4 for the November 1997 storm (Figure 4), between 1.1 and 1.5 for the September 1998 storm (Figure 5), and between 1.4 and 1.7 for the March 1999 snowmelt event (Figure 6). Because of the observed spatial variability in [Ba]/[Sr] ratios, their use in conjunction with $^{87}Sr/^{86}Sr$ should provide a greater understanding of the degree to which various soil water end-member waters contribute to storm flow.

[33] The November rain event (Figure 7a) started with an $^{87}Sr/^{86}Sr$ and [Ba]/[Sr] ratio consistent with summer base flow values. At the beginning of the storm event the

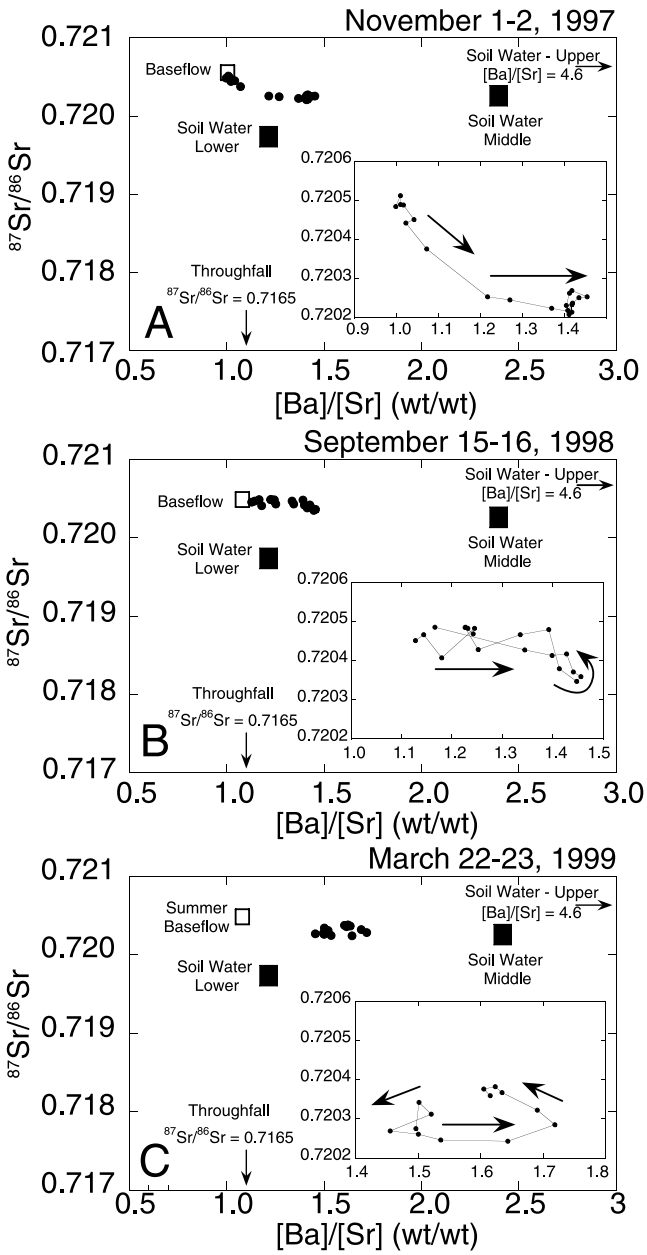

Figure 7. Storm events samples plotted on a [Ba]/[Sr]-$^{87}Sr/^{86}Sr$ end-member plot: (a) 1–2 November 1997, (b) 15–16 September 1998, (c) 22–23 March 1999. Boxes represent mean values for soil water and throughfall end-members. The inset provides an expanded view of stream water composition, with the arrows indicating the direction of change during the during the storm event.

$^{87}Sr/^{86}Sr$ ratio decreased while the [Ba]/[Sr] ratio increased, shifting stream water toward a composition similar to the lower soil water end-member. This shift is likely the result of a mixture of throughfall and soil water from both the lower and middle elevations. Later in the storm event the $^{87}Sr/^{86}Sr$ ratio remained relatively constant while the [Ba]/[Sr] ratio continued to increase, shifting the stream composition toward the middle elevation soil water, probably reflecting a decrease in throughfall contribution.

[34] The September rain event (Figure 7b) also started with the $^{87}Sr/^{86}Sr$ and [Ba]/[Sr] ratio consistent with summer base flow values, but followed a different trajectory during the event. During the first part of the storm, the [Ba]/[Sr] ratio increased while the $^{87}Sr/^{86}Sr$ ratio remained relatively constant, moving the stream water composition toward that of soil water from the middle part of the watershed. O isotopes clearly indicate that throughfall was contributing to the streamflow during this period, making it difficult to explain why the stream water value does not move toward the throughfall end-member during the early portion of the storm. Possible explanations could include a throughfall $^{87}Sr/^{86}Sr$ ratio for this storm event with an exceptionally low Sr concentration (an order of magnitude lower than the July events) or a much higher $^{87}Sr/^{86}Sr$ ratio (roughly the same as stream water). Although there is a great deal of heterogeneity within the throughfall (especially from storm to storm) and the throughfall end-member is based on measurements from a rain event the following year, it seems very unlikely to us that either scenario could provide the entire explanation for the observations. Later in the storm event, during the period of highest discharge, the $^{87}Sr/^{86}Sr$ ratio decreased while the [Ba]/[Sr] ratio increased, moving the stream composition toward a combination of soil water from the middle and lower parts of the watershed. Again, throughfall almost certainly contributed during this period of the storm. On the falling limb of the hydrograph, the stream water shifted back toward base flow values.

[35] Finally, $^{87}Sr/^{86}Sr$ and [Ba]/[Sr] ratios from the snowmelt event in March of 1999 (Figure 7c) started at a distinctly different value, which we interpret as a seasonal change in the groundwater end-member (see above). During this event, stream water first shifted toward the lower elevation soil water end-member (lower [Ba]/[Sr], lower $^{87}Sr/^{86}Sr$), then shifted toward the middle elevation soil water end-member (higher [Ba]/[Sr], same $^{87}Sr/^{86}Sr$) and finally returned to base flow values (lower [Ba]/[Sr], higher $^{87}Sr/^{86}Sr$). This pattern, of soil water from the lower watershed apparently contributing before soil water from the middle part of the watershed, may reflect the opening of shallow flow paths as thawing progressed up the watershed. Contributions from the middle and upper part of the watershed, which have higher $^{87}Sr/^{86}Sr$ ratios, may explain why the $^{87}Sr/^{86}Sr$ ratio of the stream water actually rose to a higher value than at the start of the event.

5.4. Hydrograph Separation

[36] Hydrograph separations were performed for each storm event using equations (1) and (2) with the end-members that were defined earlier. A hydrograph separation for the November storm event (Figure 8a) indicates that new water comprises 5–20% of stream water, with the greatest percent contribution occurring a few hours prior to peak discharge. Overall ~9% of storm discharge was new water (46 m^3 of 512 m^3 total discharge). Channel interception is estimated to be 31.4 m^3 based on the precipitation amount and the stream channel area (~1.5 meters wide by ~800 m long; ~1% of watershed area). This estimate is close to the total new water calculated using O isotopes and supports our assumption that most new water is derived from channel interception. Separation using Sr isotopes indicates that there is very little shallow subsurface flow until the sharp

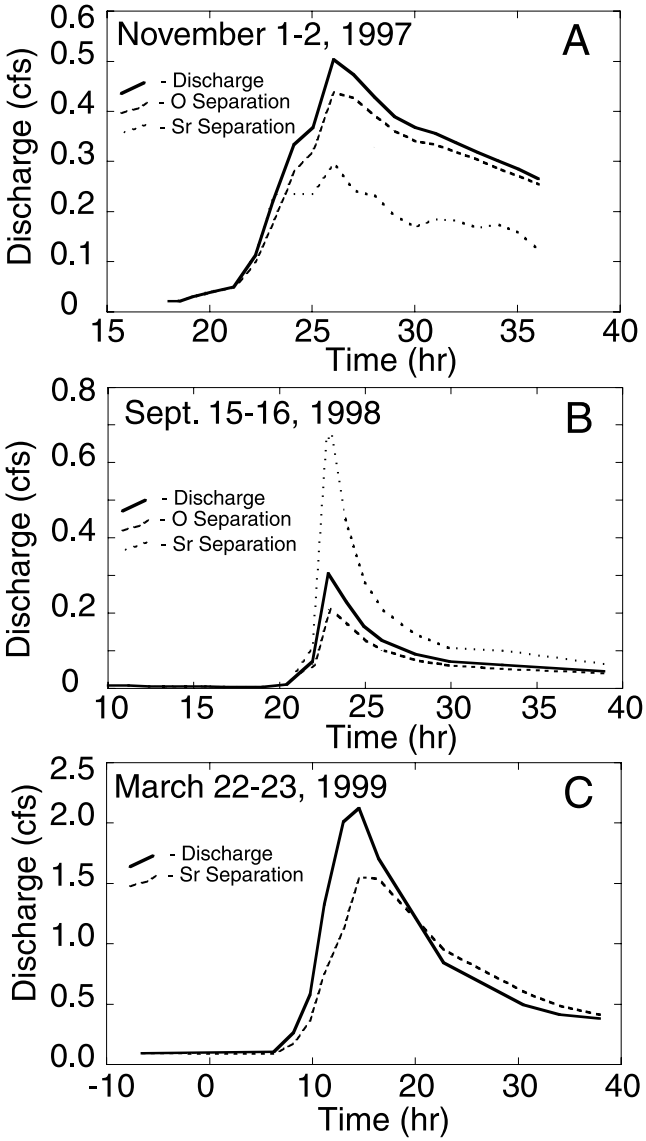

Figure 8. Results of hydrograph separation calculations: (a) 1–2 November 1997, (b) 15–16 September 1998, and (c) 22–23 March 1999. Solid line represents actual stream discharge. Dashed line represents the hydrograph separation calculated using oxygen isotopes; the area above the dashed line represents "new water," whereas below is "old water." The dotted line represents the separation calculated using Sr isotopes; the area above the dashed line represents soil water and throughfall, whereas below the line is groundwater flow. Note that the results of the Sr isotope hydrograph separation for both the September 1998 and March 1999 events produced unreasonable results; see text for discussion.

rise in stream discharge. At peak discharge shallow subsurface flow comprises ~40% of total discharge, a value which is maintained on the falling limb. Significant shallow subsurface flow at this stage of the year is consistent with higher soil moisture due to reduced transpiration as trees enter winter dormancy. This increased soil moisture provides a water source to generate shallow subsurface flow.

[37] Separation of the September 1998 storm event (Figure 8b) with oxygen isotopes indicates that between 10–30% of discharge is precipitation, with the greatest percent contribution occurring just prior to peak discharge. It is important to keep in mind that due to variation in the $\delta^{18}O$ value of precipitation during this event, there is an overestimate of the precipitation component during the early part of the storm and an underestimate for the latter part of the storm. New water was ~18% of total discharge (41.2 of 220.8 m^3) which, again, is close to the estimated amount of channel interception (45.0 m^3). Results of the hydrograph separation using Sr isotope ratios generates a result that includes negative shallow subsurface flow and groundwater flow greater than the actual stream discharge. This erroneous result is caused by both the overestimate of channel interception from the $\delta^{18}O$ separation, and also the fact that changes in stream $^{87}Sr/^{86}Sr$ do not reflect any throughfall contributions which, based on changes in $\delta^{18}O$, are clearly significant. This is well illustrated on Figure 5 in which it is observed that the greatest shift in $\delta^{18}O$ has no corresponding shift in $^{87}Sr/^{86}Sr$. The problem here is most likely with the composition of our throughfall end-member. Because we did not collect end-member samples during this storm event it is difficult to accurately constrain the throughfall composition. Potential changes in end-member compositions (i.e., very low Sr concentration; $^{87}Sr/^{86}Sr$ ratio of throughfall similar to stream water) that may resolve this problem seem highly unlikely. Although the hydrograph separation produces unreasonable results, a qualitative assessment of the changes in the $^{87}Sr/^{86}Sr$ ratio of stream water is possible. Because the total change in the $^{87}Sr/^{86}Sr$ ratio is smaller, and because this change only occurs during a brief period after peak discharge (Figure 5), one can infer that soil water makes up a significantly smaller component of the September 1998 storm compared to the November 1997 storm. The lack of shallow subsurface flow is not surprising for a storm event that occurred when trees were still actively transpiring and thus lowering soil moisture [*Likens and Bormann*, 1995]. As a result, precipitation during the growing season will enter the soil profile with some flowing quickly through macropores into the till, resulting in increased groundwater flow of old water [*McDonnell*, 1990], while the remainder enters the soil matrix but never reaches the saturation level necessary to generate shallow subsurface flow.

[38] The hydrograph of the March 1999 snowmelt event (Figure 8c), where we did not analyze $\delta^{18}O$ of stream water, was separated into shallow subsurface and groundwater flow paths using only Sr isotopes. Results indicate that soil water is a significant percentage of the storm flow on the rising limb of the hydrograph and reaches 40% immediately before peak discharge. This is in contrast to the two rain events where soil water is only significant on the falling limb of the hydrograph. On the falling limb of the snowmelt hydrograph, the $^{87}Sr/^{86}Sr$ ratio of stream water increased to values higher than at the start of the storm event. Because of this our mixing model again produces erroneous results, with deep flow contributions greater than total stream discharge. As stated earlier, we believe this is caused by increased flow from the upper portion of the watershed as thawing progressed up the watershed.

6. Conclusions

[39] Analysis of both $\delta^{18}O$ values and $^{87}Sr/^{86}Sr$ ratios for storm events indicate that these two isotopic systems yield complementary information regarding water flow paths. Although useful information is gained from our simple three end-member hydrograph separation, the methodology employed does not adequately model the system for all of the storm events studied. Limitations to the Sr isotope methodology arise due to spatial heterogeneity in the $^{87}Sr/^{86}Sr$ ratio of soil water, and the temporal variability in the $^{87}Sr/^{86}Sr$ ratio of throughfall from one storm to the next. The watershed studied here is very small (11.8 ha) and has relatively uniform crystalline bedrock and glacial till, which should minimize the chemical heterogeneity of end-member waters. However, we still observed significant spatial and temporal variability in end-member compositions, which severely limited our ability to perform three-end-member hydrograph separations. This study provides a demonstration that the use of Sr isotopes in hydrograph separations will require extensive studies of end-member water variability, even in the simplest of watersheds. Nevertheless, with selection of appropriate watershed with even lesser degrees of chemical heterogeneity in the soil and bedrock, some of the problems experienced in this study may be avoided leading to very useful multiisotope hydrograph separations. Even considering the limitations of this study, it is clear that solute isotopes ($^{87}Sr/^{86}Sr$) and solute concentration ratios ([Ca/Sr] and [Ba/Sr]) are sensitive to different hydrologic flow paths, and that they provide a wealth of information on how these flow paths change during storm events occurring during different seasons.

[40] **Acknowledgments.** JFH was supported by and EPA STAR Fellowship. Additional funding was provided by NSF grants EAR93-50632 and DEB97-26837. We thank D. White and C. Kendall for $\delta^{18}O$ analysis of waters from the November 1997 storm. A. Bailey of the USFS provided us with precipitation and stream gauge records. C. Driscoll and B. Houlton provided us with water samples from lysimeters. S. Peters, B. Klaue, A. Klaue, and W. Lee assisted in the laboratory. J. Bonin, N. Sherman, and E. Hughey assisted with sample collection. S. Bailey, D. Buso, G. Likens, C. Driscoll, and B. Dresser provided valuable insight and background information about the watershed. This is a contribution of the Hubbard Brook Ecosystem Study. This research was conducted at the Hubbard Brook Experimental Forest, which is owned and operated by the Northeastern Research Station, USDA Forest Service, Newtown Square, PA.

References

Albarede, F., *Introduction to Geochemical Modeling*, Cambridge Univ. Press, New York, 1995.

Bailey, S. W., J. W. Hornbeck, C. T. Driscoll, and H. E. Gaudette, Calcium inputs and transport in a base-poor forest ecosystem as interpreted by Sr isotopes, *Water Resour. Res.*, *32*, 707–719, 1996.

Bain, D. C., A. J. Midwood, and J. D. Miller, Strontium isotope ratios in streams and the effect of flow rate in relation to weathering in catchments, *Catena*, *32*, 143–151, 1998.

Barton, C. C., Bedrock geologic map of Hubbard Brook Experimental Forest and maps of fractures and geology in roadcuts along Interstate 93, Grafton County, New Hampshire, *Geol. Map 0160-0753*, U.S. Geol. Surv., Reston, Va., 1997.

Bencala, K. E., Interactions of solutes and streambed sediment: 2. A dynamic analysis of coupled hydrologic and chemical processes that determine solute transport, *Water Resour. Res.*, *20*, 1804–1814, 1984.

Bencala, K. E., V. C. Kennedy, G. W. Zellweger, A. P. Jackman, and R. J. Avanzino, Interactions of solutes and streambed sediment: 1. An experimental analysis of cation and anion transport in a mountain stream, *Water Resour. Res.*, *20*, 1797–1803, 1984.

Blum, J. D., E. H. Taliaferro, M. T. Weisse, and R. T. Holmes, Changes in Sr/Ca. Ba/Ca and $^{87}Sr/^{86}Sr$ ratio between trophic levels in two forest ecosystems in the northeastern USA, *Biogeochemistry*, *49*, 87–101, 2000.

Blum, J. D., A. Klaue, C. A. Nezat, C. T. Dricoll, C. E. Johnson, T. G. Siccama, C. Eagar, T. J. Fahey, and G. E. Likens, Mycorrhizal weathering of apatite as an important Ca source in base-poor forest ecosystems, *Nature*, *417*, 729–731, 2002.

Bullen, T. D., and C. Kendall, Tracing of weathering reactions and water flowpaths: A multi-isotope approach, in *Isotope Tracers in Catchment Hydrology*, edited by C. Kendall and J. J. McDonnell, pp. 611–646, Elsevier Sci., New York, 1998.

Dewalle, D. R., and B. R. Sharpe, Three-component tracer model for stormflow on a small Appalachain forested catchment, *J. Hydrol.*, *104*, 301–310, 1988.

Dunne, T., Field studies of hillslope flow processes, in *Hillslope Hydrology*, edited by M. J. Kirkby, pp. 227–293, Wiley-Interscience, New York, 1978.

Dunne, T., Models of runoff processes and their significance, in *Scientific Basis of Water Resources Management*, pp. 17–30, Natl. Acad. Press, Washington, D.C., 1982.

Dunne, T., and R. D. Black, Partial area contributions to storm runoff in a small New England watershed, *Water Resour. Res.*, *6*, 1296–1311, 1970.

Federer, C. A., L. D. Flynn, C. W. Martin, J. W. Hornbeck, and R. S. Pierce, *Thirty Years of Hydrometric Data at the Hubbard Brook Experimental Forest, New Hampshire*, *Gen. Tech. Rep. U.S. Dep. Agric., NE-141*, 1990.

Genereux, D. P., and H. F. Hemond, Three-component tracer model for stormflow on a small Appalachain forested catchment-comment, *J. Hydrol.*, *117*, 377–380, 1990.

Genereux, D. P., and R. P. Hooper, Oxygen and hydrogen isotopes in rainfall-runoff studies, in *Isotope Tracers in Catchment Hydrology*, edited by C. Kendall and J. J. McDonnell, pp. 319–346, Elsevier Sci., New York, 1998.

Hall, R. O., K. H. MacNeale, E. S. Bernhardt, and M. Field, Biogeochemical responses of two forest streams to a 2-month calcium addition, *Freshwater Biol.*, *46*, 291–302, 2001.

Hewlett, J. D., and A. R. Hibbert, Factors affecting the response of small watersheds to precipitation in humid areas, in *Forest Hydrology*, edited by W. E. Sopper and W. L. Lull, pp. 275–290, Pergamon, New York, 1967.

Hooper, R. P., and C. A. Shoemaker, A comparison of chemical and isotopic hydrograph separation, *Water Resour. Res.*, *22*, 1444–1454, 1986.

Hooper, R. P., N. Christophersen, and N. E. Peters, Modelling streamwater chemistry as a mixture of soilwater end—members-An application to the Panola Mountain Catchment, Georgia, USA, *J. Hydrol.*, *116*, 321–343, 1990.

Hornberger, G. M., J. P. Raffensperger, P. L. Wiberg, and K. N. Eshleman, *Elements of Physical Hydrology*, Johns Hopkins Univ. Press, Baltimore, Md., 1998.

Johnson, C. E., C. T. Driscoll, T. G. Siccama, and G. E. Likens, Element fluxes and landscape position in a northern hardwood forest watershed ecosystem, *Ecosystems*, *3*, 159–184, 2000.

Kendall, C., M. G. Sklash, and T. D. Bullen, Isotope tracers of water and solute sources in catchments, in *Solute Modelling in Catchment Systems*, edited by S. T. Trudgill, pp. 261–303, John Wiley, Hoboken, N.J., 1995.

Kirchner, J. W., X. Feng, and C. Neal, Fractal stream chemistry and its implications for contaminant transport in catchments, *Nature*, *403*, 524–527, 2000.

Land, M., J. Ingri, P. S. Andersson, and B. Ohlander, Ba/Sr, Ca/Sr, $^{87}Sr/^{86}Sr$ ratios in soil water and groundwater: Implications for relative contributions to stream discharge, *Appl. Geochem.*, *15*, 311–325, 2000.

Land, M., and B. Ohlander, Seasonal variations in the geochemistry of shallow groundwater hosted in granitic till, *Chem. Geol.*, *143*, 205–216, 1997.

Landon, M. K., G. N. Delin, S. C. Komor, and C. P. Regan, Comparison of the stable-isotopic composition of soil water collected from suction lysimters, wick samples, and cores in a sandy insaturated zone, *J. Hydrol.*, *224*, 45–54, 1999.

Likens, G. E., and F. H. Bormann, *Biogeochemistry of a Forested Ecosystem*, 2nd ed., Springer-Verlag, New York, 1995.

McDonnell, J., A rationale for old water discharge through macropores in a steep, humid catchment, *Water Resour. Res.*, *26*, 2821–2832, 1990.

McDonnell, J. J., M. K. Stewart, and I. F. Owens, Effect of catchment-scale subsurface mixing on stream isotopic response, *Water Resour. Res.*, *27*, 3065–3073, 1991.

Miller, E. K., J. D. Blum, and A. J. Friedland, Determination of soil exchangeable-cation loss and weathering rates using Sr isotopes, *Nature*, *362*, 438–441, 1993.

Miller, W. R., and J. I. Drever, Water chemistry of a stream following a storm, Absaroka Mountains, Wyoming, *Geol. Soc. Am. Bull.*, *88*, 286–290, 1977.

Ogunkoya, O. O., and A. Jenkins, Analysis of storm hydrograph and flow pathways using a three-component hydrograph separation model, *J. Hydrol.*, *142*, 71–88, 1993.

Pearce, A. J., M. K. Strewart, and M. G. Sklash, Storm runoff generation in humid headwater catchments: 1. Where does the water come from?, *Water Resour. Res.*, *22*, 1263–1272, 1986.

Pierce, R. S., Evidence for overland flow on forest watersheds, in *Forest Hydrology*, edited by W. E. Sopper and H. W. Lull, pp. 247–252, Pergamon, New York, 1967.

Rice, K. C., and G. M. Hornberger, Comparison of hydrochemical tracers to estimate source contributions to peak flow in a small, forested, headwater catchment, *Water Resour. Res.*, *34*, 1755–1766, 1998.

Simonetti, A., C. Gariepy, and J. Carignan, Pb and Sr isotopic evidence for sources of atmospheric heavy metals and their deposition budgets for northeastern North America, *Geochim. Cosmochim. Acta*, *64*, 3439–3452, 2000.

Sklash, M. G., M. K. Strewart, and A. J. Pearce, Storm runoff generation in humid headwater catchments: 2. A case study of hillslope and low-order stream response, *Water Resour. Res.*, *22*, 1273–1282, 1986.

J. D. Blum, Department of Geological Sciences, University of Michigan, Ann Arbor, MI 48109, USA.

J. F. Hogan, Department of Hydrology and Water Resources, University of Arizona, Tucson, AZ 85721, USA. (jhogan@hwr.arizona.edu)